PROJECTION OF THE SOLIDUS SURFACE AND REACTIONS ON THE SOLIDIFICATION OF ALLOYS OF THE Ti–Zr–Ni SYSTEM IN THE REGION Ti–TiNi–ZrNi–Zr

V.N. Eremenko, E.L. Semenova, and L.A. Tret'yachenko

Izvestiya Rossiiskoi Akademii Nauk. Metally,
No. 6, pp. 138-143, 1992

UDC 669.01.24'295'96'.669.017.3

The phase equilibria of the Ti–Zr–Ni system were studied for the first time in the region up to 50 at. % of Ni. The solidus and liquidus surfaces and the schemes of transformation in solidification were plotted.

Phase equilibria in the ternary Ti–Zr–Ni system were not studied previously. A ternary Laves phase (λ_1) with a type $MgZn_2$ structure was discovered in an alloy with an equiatomic composition [1]. Study of the phase equilibria in the region Ti–TiNi–ZrNi–Zr at 700 °C performed by the authors confirmed the existence of this phase [2]. The λ_1 phase was found to have a region of homogeneity within 14–33 at. % of Zr and 27-38 at. % of Ni and is in equilibrium with all the phases existing at 700 °C in the limiting binary systems up to 50 at. % of Ni.

The present report gives the results of studying the structure of the alloys at subsolidus temperatures and the phase transformations in the Ti–TiNi–ZrNi–Zr region. The alloys to be studied were melted in an arc furnace in argon from iodide titanium and zirconium and Grade H–1 nickel and were studied in the as-cast and annealed state by microstructural, X-ray, differential thermal, and local X-ray spectral analyses.

The binary systems confining the part of the ternary Ti-Zr-Ni phase diagram being studied are characterized in the subsolidus region by the existence of a continuous series of solid solutions (β) of the compounds TiNi, Ti_2Ni, ZrNi, and Zr_2Ni between the high-temperature modifications of titanium and zirconium. Information on the crystalline structure and ways of phase formation is given in Table 1.

Study of the structure of the section TiNi–ZrNi confining the part of the phase diagram of the ternary Ti–Zr–Ni system being considered showed it to be pseudobinary of the peritectic type [7].

Triangulation of the ternary Ti–Zr–Ni system over this section enables one to consider equilibrium in the region Ti–TiNi–ZrNi–Zr regardless of the equilibria in the remaining part of the phase diagram.

The phase equilibria in the binary confining systems are described in Table 2.

At the solidus temperatures, as at 700 °C, equilibria of the Laves phase λ_1 with all the phases of the binary systems in the subsolidus regions exist.

The solidus is formed by the surfaces of the beginning of melting of the phases based on the binary compounds TiNi (δ_1), ZrNi (δ_2), Ti_2Ni (η), and Zr_2Ni (θ), the solid solutions (Ti, Zr) (β) and the ternary Laves phase (λ_1), the planes of the conodal triangles corresponding to the beginning of melting of the alloys in the region of three-phase equilibria ($\beta + \eta + \lambda_1$, $\eta + \delta_1 + \lambda_1$, $\delta_1 + \delta_2 + \lambda_1$, $\delta_2 + \theta + \lambda_1$, $\beta + \theta + \lambda_1$), and linear surfaces of the beginning of melting of the alloys in the two-phase regions ($\beta + \lambda_1$, $\beta + \eta$, $\beta + \theta$, $\lambda_1 + \delta_1$, $\lambda_1 + \delta_2$, $\lambda_1 + \theta$, $\delta_1 + \eta$, $\delta_1 + \delta_2$, $\delta_2 + \theta$, $\lambda_1 + \eta$).

Some features of individual elements of the solidus surface in the region being considered must be noted, namely, (1) the linear surface of the solidus of the region $\delta_1 + \lambda_1$ has a temperature peak at 925 °C from which it drops smoothly to both sides down to 880 °C; (2) the linear surface $\delta_1 + \delta_2$ drops steeply from 1160 °C in the cross section TiNi–ZrNi to 880 °C at about 49 at. % Ni, and expands from 2 at. % (46–48 at. % of Zr) to about 16 at. % (31–47 at. % of Zr); and (3) the melting point of the phase λ_1 increases with a growth in the nickel content from 770 to 925 °C, its homogeneity region at the solidus temperatures is within about 22-32 at. % of Zr and 28-38 at. % of Ni.

A projection of the liquidus surface and a diagram of the phase transformations in crystallization are presented in Fig. 1. The liquidus is formed by surfaces of primary crystallization of the phases λ_1, β, η, δ_1, δ_2, and θ that are separated by boundary lines corresponding to the composition of the liquid phases participating in the monovariant processes of solidification of the two-phase alloys: P_3dP_1 is the congruent

Table 1

Solid Phases in Region Ti–TiNi–ZrNi–Zr of Ternary Ti–Ni–Zr System at Subsolidus Temperatures

Phase	Structural type, prototype	Lattice constants, nm	Remarks
$TiNi(h)$, δ_1 ≥ 60 °C	B2, CsCl	a = 0.298 a = 0.304 a = 0.305 a = 0.306	[3]. Melts congruently at 1310 °C [4]. Dissolves up to 46% Zr at 1160 °C and 50% Ni 50% Ni, 6% Zr 50% Ni, 10% Zr 50% Ni, 20% Zr
Ti_2Ni, η	Ti_2Ni	a = 1.133 a = 1.137	[3]. Forms by peritectic reaction at 984 °C [4]. Dissolves up to 8% Zr at 33.3% Ni 33.3% Ni, 5% Zr
$(Ti, Zr)(h)$, β	A2, W	a = 0.33065 a = 0.36090	β-Ti [5] β-Zr [5]
$ZrNi$, λ_2	B_f, CrB	a = 0.3268 b = 0.9937 c = 0.41021 a = 0.323 b = 0.991 c = 0.412	Melts congruently at 1260 °C [6]. Dissolves up to 2% Ti at 1160 °C 50% Ni, 48% Zr
Zr_2Ni, θ	C16, $CuAl_2$	a = 0.649 c = 0.527 a = 0.648 c = 0.524	Melts congruently at 1120 °C [6] 33.3% Ni, 62.5% Zr
$(TiZrNi)$, λ_1	C14, $MgZn_2$	a = 0.517 c = 0.844 a = 0.519 c = 0.850	Dissolves about 7% Ti Region of homogeneity 22-32% Zr, 28-38% Ni 33.3% Ni, 26.7% Zr 33.3% Ni, 33.3% Zr

Note. All the percentages are atomic ones.

Table 2

Nonvariant Reactions in the Systems Confining the Region Ti–TiNi–ZrNi–Zr in Solidification

System	Reaction	T, °C	Type, remarks
Ti–Ni	$TiNi + L \rightleftarrows Ti_2Ni$	984	Peritectic [3]
	$L \rightleftarrows Ti_2Ni + \langle\beta\text{-Ti}\rangle$	945	Eutectic [3]
Zr–Ni	$L \rightleftarrows ZrNi + Zr_2Ni$	1010	Eutectic [6]
	$L \rightleftarrows Zr_2Ni + \langle\beta + Zr\rangle$	960	Ditto
Ti–Zr	$L \rightleftarrows \langle\beta\text{-Ti, Zr}\rangle$	1540±15	Minimum at 38.2 at. % Zr [4]
TiNi–ZrNi	$L + \langle Zr, Ni\rangle \rightleftarrows \langle TiNi\rangle$	1160	Peritectic (the present report) [7]
	$L \rightleftarrows (Ti, Zr)Ni$	1100	Minimum at 25 at. % Zr (the present report) [7]

process $L \rightleftarrows \delta_1 + \lambda_1$ on section dP_1, incongruent process $L + \delta_1 \rightleftarrows \lambda_1$ is on section dP_3 (both are within the interval of 925-880 °C); P_1P_2 is the congruent process $L \rightleftarrows \delta_1 + \lambda_1$, 880-830 °C; P_2E is the process $L \rightleftarrows \lambda_1 + \theta$, 880-770 °C; P_3P_4 is the process $L \rightleftarrows \eta + \lambda_1$, 880-810 °C; P_4E is the process $L \rightleftarrows \beta + \lambda_1$, 810-770 °C; p_1P_1 is for 1160-880 °C; the incongruent process $L + \delta_2 \rightleftarrows \delta_1$ is replaced by the congruent one $L \rightleftarrows \delta_1 + \delta_2$; e_1P_2 is the process $L \rightleftarrows \delta_2 + \theta$, 1010-830 °C; e_2E is the process $L \rightleftarrows \beta + \theta$, 960-770 °C; p_2P_3 is for 984-830 °C; the incongruent process $L + \delta_1 \rightleftarrows \eta$ is replaced by the congruent one $L \rightleftarrows \delta_1 + \eta$; e_3P_4 is the process $L \rightleftarrows \beta + \eta$, 945-810 °C.

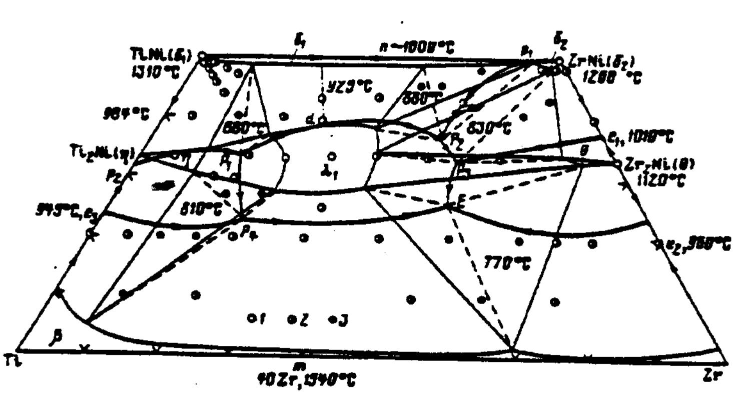

Fig. 1. Projection of liquidus surface and diagram of phase transformations in solidification of alloys of the Ti–Zr–Ni system in the region Ti–TiNi–ZrNi–Zr:
1—single-phase alloys; 2—two-phase alloys; 3—three-phase alloys.

The intersection of these boundary curves yields five points corresponding to the composition of the liquid in equilibrium with the solid phases at the temperatures of the four-phase nonvariant equilibria described in Table 3.

The phase transformations in solidification of the alloys of the ternary Ti–Zr–Ni system in the region Ti–TiNi–ZrNi–Zr is shown in Fig. 2.

Table 3

Nonvariant Reactions in the Region Ti–TiNi–ZrNi–Zr in Solidification

Reaction	T, °C	Type	Phase	Phase composition, at. % Ni	Phase composition, at. % Zr
$L+(\delta_1) \rightleftarrows \lambda_1+\delta_1$	925		L, λ_1(d)	38	22
			δ_1	49	17
			λ_1	37	16
			η	34	6
$L+\delta_1 \rightleftarrows \lambda_1+\eta$	880	Peritectic	L	P_3	
			δ_1	49	7
			λ_1	37	16
			η	34	6
$L+\delta_1 \rightleftarrows \delta_2+\lambda_1$	880	Ditto	L	P_1	
			δ_1	49	31
			δ_2	49	47
			λ_1	38	30
$L+\delta_2 \rightleftarrows \lambda_1+\theta$	830	Ditto	L	P_2	
			δ_2	49	49
			λ_1	33	33
			θ	33	60
$L+\eta \rightleftarrows \beta+\lambda_1$	810	Ditto	L	P_4	
			η	31	9
			β	4.5	7.6
			λ_1	28	22
$L \rightleftarrows \beta+\lambda_1+\theta$	770	Eutectic	L	E	
			β	1.5	69
			λ_1	29	33
			θ	32	62

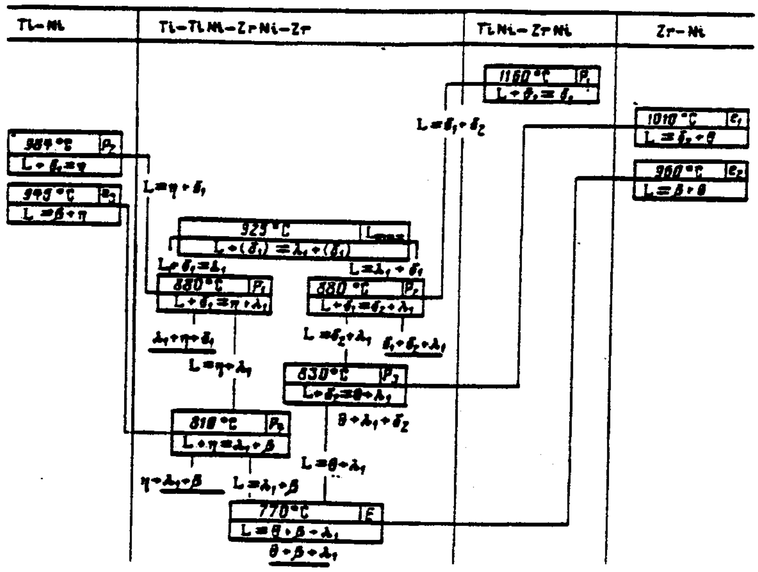

Fig. 2. Phase transformations in the solidification of alloys of the Ti–Zr–Ni system in the region Ti–TiNi–ZrNi–Zr.

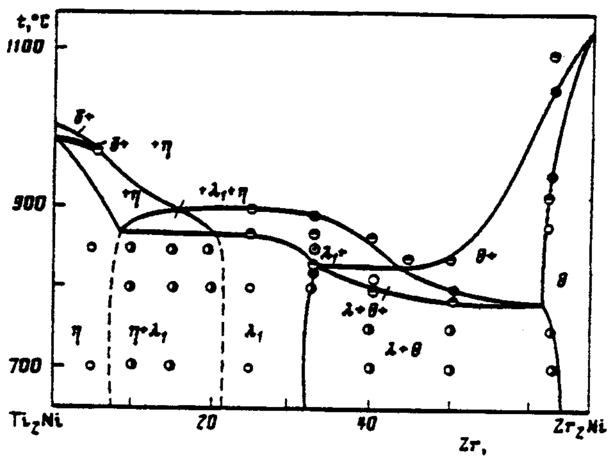

Fig. 3. Polythermal section of the Ti–Zr–Ni system along the isoconcentrate 33.3 at. % Ni.

In almost the entire region of compositions, the phase λ_1 solidifies from a melt (Fig. 3).

Figure 4 shows the microstructure of selected alloys Ti–Zr–Ni.

The solidification of binary eutectic mixtures and the ternary eutectic within a broad concentration and small temperature intervals at temperatures relatively low in comparison with binary systems creates conditions favorable for producing amorphous alloys.

REFERENCES

1. M.Yu. Teslyuk, Metal Compounds with Laves Phase Structures, Nauka, Moscow, 1969.
2. V.N. Eremenko, E.L. Semenova, and L.A. Tretyachenko, Dokl. AN Ukr. SSR. Ser. A, no. 2, p. 79, 1988.

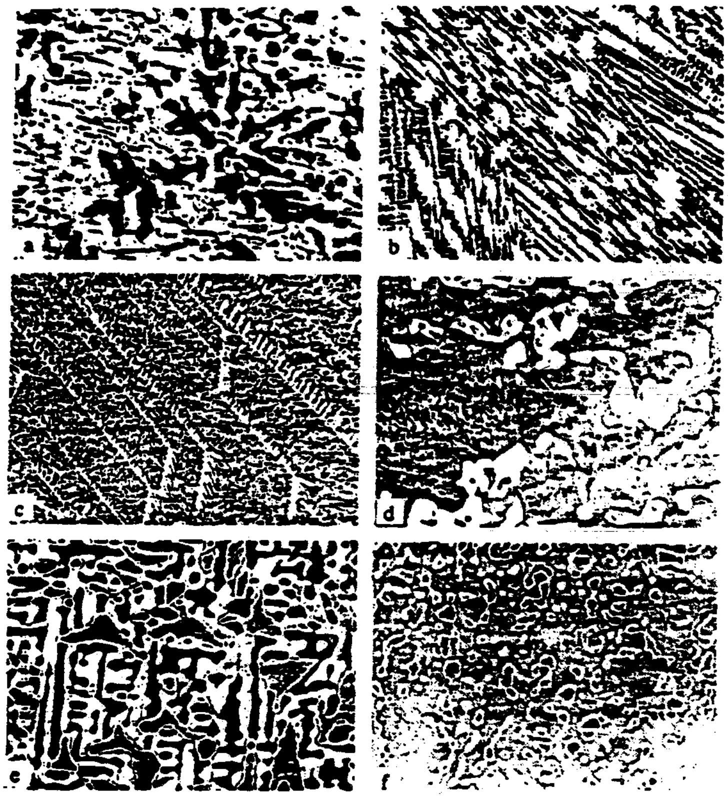

Fig. 4. Microstructure of the Ti–Zr–Ni alloys:
(a) 20 at. % Ni-40 at. % Zr–Ti, as-cast, ×1000, β + eut. ($\beta + \lambda_1$);
(b) 33.3 at. % Ni-10 at. % Zr–Ti, as-cast, ×200, $\eta + \lambda_1$;
(c) 33.3 at. % Ni-40 at. % Zr–Ti, as-cast, ×100, $\lambda_1 + (\lambda_1 + \theta)$;
(d) 10 at. % Ni-10 at. % Zr–Ti, 800 °C, ×500, $\beta + \lambda_1 + \eta$;
(e) 40 at. % Ni-10 at. % Zr–Ti, 850 °C, ×1000, $\delta_1 + \lambda_1 + \eta$;
(f) 45 at. % Ni-33.3 at. % Zr–Ti, 800 °C, ×1500, $\delta_1 + \lambda_1 + \delta_2$

3. P. Rogl, In: Atomic Energy Rev. Vienna, IAEA, Spec. Issue no. 9, p. 201, 1983.
4. O.Kubashewski and O. von Goldbeck, In: Atomic Energy Rev. Vienna, IAEA, Spec. Issue no.9, p. 199, 1983.
5. T.B. Massalski (ed.), Binary Alloy Phase Diagrams, Metals Park, Ohio, ASW, 1986.
6. P. Nash and C.S. Jayanth, Bull. Alloy Phase Diagr., vol. 5, no. 2, p. 144, 1984.
7. V.N. Eremenko, E.L. Semenova, L.A. Tretyachenko, and Z.G. Domatyrko, Izv. Vuzov. Tsv. Metallurgiya, no. 6, p. 85, 1989.

April 24, 1992 Kiev